

Influence of Doping on the Magnetic Properties and Local Microstructures in Fe-Doped YMnO₃

Xiaopeng Ge¹, Jiaou Wang², Kurash Ibrahim², Wenbo Yang¹, Xueguang Dong¹, Qi Li^{1*}

¹Department of Physics, Southeast University, Nanjing, China

²Beijing Synchrotron Radiation Facility, Institute of High Energy Physics, Chinese Academy of Sciences, Beijing, China

Email: * qli@seu.edu.cn

Received 25 November 2014

Abstract

Polycrystalline YMn_{1-x}Fe_xO₃ (0 < x < 0.1) samples are synthesized by solid-state reaction method and characterized by X-ray diffraction. The X-ray diffraction patterns indicate that YMn_{1-x}Fe_xO₃ compounds maintain hexagonal structure with space group of P6₃cm. Ferromagnetism of YMn_{1-x}Fe_xO₃ increases with increasing doping concentration of Fe³⁺, attributed to the suppression of the frustration and the change of the Mn-O bond length certificated by XAS analysis.

Keywords

Multiferroics, YMn_{1-x}Fe_xO₃, Hybrid States, X-Ray Absorption Spectra

1. Introduction

Multiferroic materials simultaneously possess magnetic and ferroelectric orders which co-exist and couple with each other [1]. They are able to put the electrical, magnetic and optical properties together and suitable to design new multi-functional electronic information storage elements. Multiferroic materials have become one of the most active areas in the field of materials science. Hexagonal RMnO₃ (R = Y, Ho-Lu) materials occupy a very important position in the single-phase multiferroic materials. They have novel properties, indicating the potential in the material research and applications [2]. Therefore hexagonal manganites YMnO₃ have attracted widespread attention in recent years. However, because YMnO₃ exhibits the coupling of antiferromagnetism and ferroelectricity, such multiferroic is not very sensitive to the applied external electromagnetic fields [3]; thereby it is the purpose of many researchers to increase the ferromagnetic property of YMnO₃.

As an effective research tool, ion doping in A site (*i.e.* Y site) or B site (*i.e.* Mn site) of YMnO₃ is often used to change the ferromagnetic property of YMnO₃ [4]. Some research teams have selected kinds of ions replacing the Y³⁺ to modulate the antiferromagnetic order of YMnO₃, such as Lu³⁺, Sr²⁺. It will make partial antiferromagnetic order convert to ferromagnetic properties in the compounds where Y³⁺ was replaced by Lu³⁺ or Sr²⁺ [5]

*Corresponding author.

[6]. Transition metal ions replacing the Mn^{3+} in the B site of YMnO_3 is another way to modulate the antiferromagnetic order. Several current experiments have successfully synthesized samples in which the Mn^{3+} in the B site of YMnO_3 is replaced by kinds of ions, such as Fe^{3+} , Al^{3+} , Cu^{2+} , Ti^{3+} , etc. [7]-[10]. Y. J. Yoo *et al.*, who have synthesized polycrystalline Cr-doped YMnO_3 with hexagonal structure and space group $\text{P6}_3\text{cm}$, found that the magnetic transition temperature increased as the concentration of Cr increased [11]. Indeed, it will make the ferromagnetic property of YMnO_3 increase significantly by the substitution of the Mn^{3+} with transition metal ions in the YMnO_3 samples. However, the reason of the change of magnetism is still not explained clearly. Compared to previous studies about YMnO_3 samples, this paper will explain the change of magnetism when the Fe^{3+} replaces the Mn^{3+} in the B site of YMnO_3 samples according to XAS of O K edge and Mn L edge.

2. Experimental Details

Polycrystalline $\text{YMn}_{1-x}\text{Fe}_x\text{O}_3$ ($0 < x < 0.1$) samples were prepared by a standard solid-state reaction. The analytical pure Y_2O_3 , MnO_2 and Fe_2O_3 were weighed according to stoichiometric proportion. The mixed powder was put into an agate mortar milling 5 hours with petroleum ether. The milled powder was transferred into a corundum crucible in a tube furnace. The powder was sintered 2 h at 1100°C then heated to 1370°C , maintaining 24 hours. Taking out the powder and milling for 2 hours, we can obtain the $\text{YMn}_{1-x}\text{Fe}_x\text{O}_3$ ($0 < x < 0.1$) samples. The crystal structures of the samples were examined by X-ray diffraction (XRD) with $\text{Cu K}\alpha$ radiation (Rigaku Smart Lab3, Japan). The magnetic properties of $\text{YMn}_{1-x}\text{Fe}_x\text{O}_3$ were measured by SQUID-VSM (Quantum Design, USA). In order to observe the change of Y-O, Mn-O hybrid states, the X-ray absorption spectroscopy (XAS) of O K edge and Mn L edge of $\text{YMn}_{1-x}\text{Fe}_x\text{O}_3$ ($0 < x < 0.1$) samples were measured utilizing total electron yield (TEY) mode in photoemission spectroscopy experiment station of Beijing Synchrotron Radiation Facility, Chinese Academy of Sciences.

3. Results and Discussion

XRD patterns of powder samples $\text{YMn}_{1-x}\text{Fe}_x\text{O}_3$ ($0 < x < 0.1$) at room temperature are measured as shown in **Figure 1**. XRD patterns of $\text{YMn}_{1-x}\text{Fe}_x\text{O}_3$ illustrate that all samples are in single phase with hexagonal lattice structure, space group $\text{P6}_3\text{cm}$. It illustrates that Fe^{3+} ion replaces the lattice position of Mn^{3+} ion and doesn't change the lattice structures of $\text{YMn}_{1-x}\text{Fe}_x\text{O}_3$ samples, with the incorporation of Fe^{3+} ion. Because Fe^{3+} ionic radius (0.49 \AA) is smaller than the Mn^{3+} ionic radius (0.58 \AA), the lattice structures of $\text{YMn}_{1-x}\text{Fe}_x\text{O}_3$ samples have a slight contraction. This change can be found from the diffraction peaks of $\text{YMn}_{1-x}\text{Fe}_x\text{O}_3$ samples. The diffraction peak (112) of $\text{YMn}_{0.95}\text{Fe}_{0.05}\text{O}_3$ shifts toward the higher angle with respect to that of YMnO_3 (as inset of **Figure 1**). The contraction of lattice structure will lead to the change of Y-O, Mn-O hybrid states and Y, Mn ligand structure, which will affect the bond lengths of Y-O and Mn-O. These changes will affect the magnetic order of $\text{YMn}_{1-x}\text{Fe}_x\text{O}_3$ ($0 < x < 0.1$) samples.

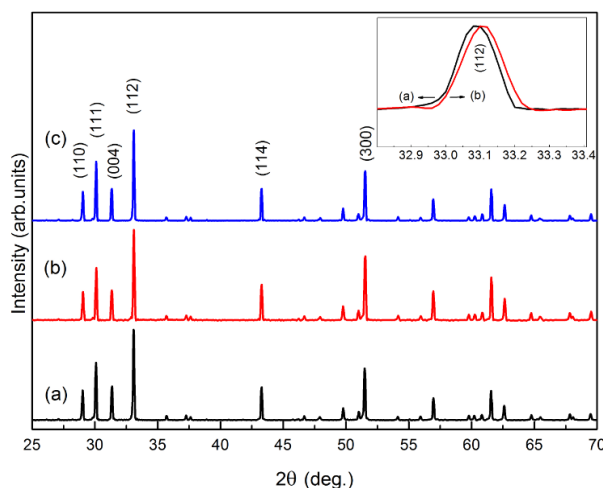


Figure 1. XRD patterns of $\text{YMn}_{1-x}\text{Fe}_x\text{O}_3$ ($0 < x < 0.1$) samples. (a) $x = 0$; (b) $x = 0.05$; (c) $x = 0.08$.

In order to observe the magnetism change of $YMn_{1-x}Fe_xO_3$ samples, field cooled (FC) temperature dependent magnetization (M - T) curves were measured from 30 K to 300 K with cooling field of 5000 Oe as shown in **Figure 2**. The magnetism of $YMn_{1-x}Fe_xO_3$ samples are significantly enhanced, which is attributed to the incorporation of Fe^{3+} ion. Since Mn trimer arrangement exists the magnetic frustration effect (shown in **Figure 2(b)**), the magnetic frustration effect is relieved when Fe^{3+} ions partially replace Mn^{3+} ions in the B-site of crystal lattice. And Fe^{3+} ion having five 3d electrons will enhance the magnetism of $YMn_{1-x}Fe_xO_3$ samples. In addition, due to Fe^{3+} ions doping, the lattice structures of $YMn_{1-x}Fe_xO_3$ samples shrink slightly, causing the magnetic exchange interaction to be enhanced.

Figure 3 shows the XAS of O K edge of $YMn_{1-x}Fe_xO_3$ samples which illustrate the hybrid states between O 2p and Mn 3d, Y 4d, Mn 4sp/Y 5sp. The absorption spectra of the O 2p-Mn 3d hybrid states can be refined to four peaks, namely $a_{1g}\uparrow$, $e_{1g}\downarrow$, $e_{2g}\downarrow$, $a_{1g}\downarrow$ [12]. O 2p-Y 4d electron orbitals also have a strong hybridization as shown by the XAS of O K edge. Mn^{3+} ion is surrounded by 5 Oxygen atoms, forming bipyramid structure MnO_5 , as shown in **Figure 4(a)**.

The ferroelectric transition temperature T_C of $YMnO_3$ is about 900 K. When paraelectric phase is transformed to ferroelectric phase for $YMnO_3$, the bipyramid MnO_5 will be tilted, as shown in **Figure 4(b)** [13]. The ferro-

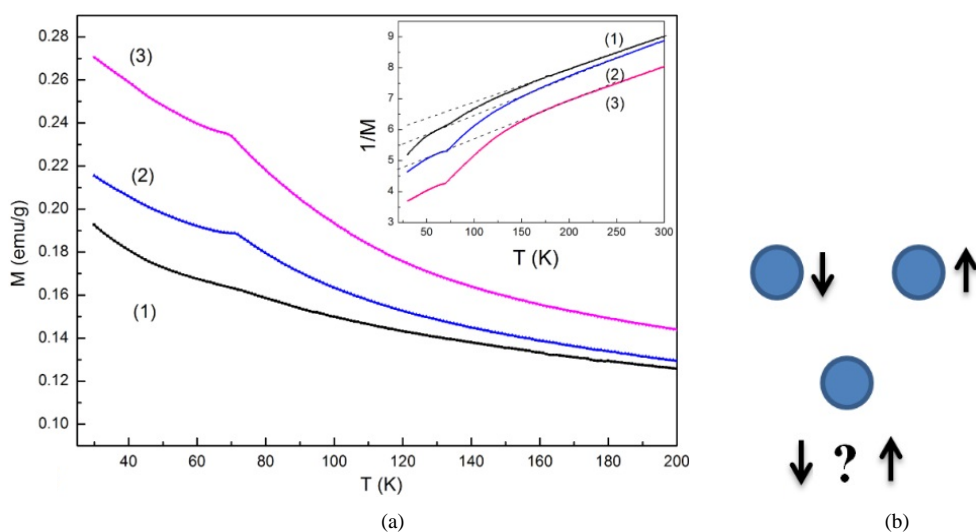


Figure 2. (a) The field cooled (FC) temperature dependent magnetization (M - T) curves of $YMn_{1-x}Fe_xO_3$ ($0 < x < 0.1$) samples. (1) $x = 0$, (2) $x = 0.05$, (3) $x = 0.08$; (b) Schematic diagram of the magnetic frustration effect in Mn trimer arrangement of $YMnO_3$.

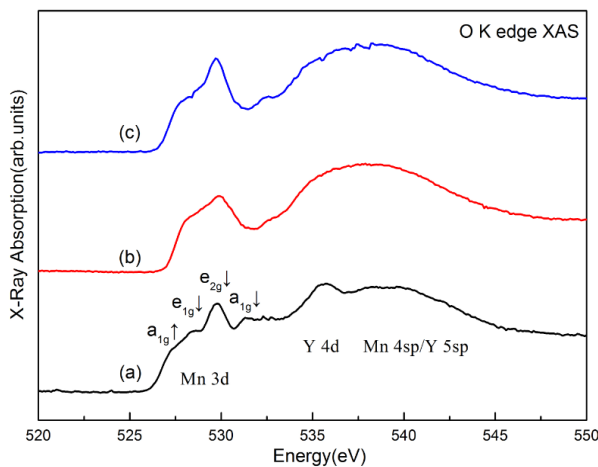


Figure 3. The X-ray absorption spectroscopy (XAS) of O K edge of $YMn_{1-x}Fe_xO_3$ ($0 < x < 0.1$) samples. (a) $x = 0$; (b) $x = 0.05$; (c) $x = 0.08$.

lectric order of YMnO_3 is induced by the inclined bipyramid MnO_5 which leads to the orbital hybridization of O 2p-Y 4d enhanced. As shown in **Figure 3**, due to Fe^{3+} ion doped, the intensity of $e_{1g}\downarrow$ and $e_{2g}\downarrow$ peaks are enhanced which indicates the orbital hybridization of O 2p-Mn 3d is enhanced. The change in the intensity of $e_{1g}\downarrow$ and $e_{2g}\downarrow$ peaks also shows that the structural distortion of MnO_5 has been minorly changed. The structural distortion of MnO_5 will also affect the coordination environment of Y^{3+} ion, resulting in the change of O 2p-Y 4d orbital hybridization. The absorption spectra of O 2p-Y 4d are enhanced in intensity, as shown in **Figure 3**, consistent with our discussion.

Because O 2p-Mn 3d orbital hybridization is changed, the electronic orbital of Mn 3d presents a more complex structure in $\text{YMn}_{1-x}\text{Fe}_x\text{O}_3$ ($0 < x < 0.1$) samples. The electronic orbital of Mn 3d splits into e_{1g} , e_{2g} , a_{1g} (as shown in **Figure 4(c)**) [12]. As shown in **Figure 5**, the lower energy segments of Mn 3d L_3 absorption spectra peak are significantly enhanced in $\text{YMn}_{0.95}\text{Fe}_{0.05}\text{O}_3$ and $\text{YMn}_{0.92}\text{Fe}_{0.08}\text{O}_3$ samples compared to that of YMnO_3 sample. This shows that there are more empty electronic states in the low energy states (such as e_{1g} , e_{2g}), due to Fe^{3+} doping, which is consistent with the situation of O K edge absorption spectra. The electronic orbital of Mn 3d is closely related to magnetic exchange interaction and lattice distortion of MnO_5 .

4. Conclusion

Polycrystalline $\text{YMn}_{1-x}\text{Fe}_x\text{O}_3$ ($0 < x < 0.1$) samples were prepared by a standard solid-state reaction. The lattice structures of hexagonal $\text{YMn}_{1-x}\text{Fe}_x\text{O}_3$ ($0 < x < 0.1$) samples are unchanged with Fe^{3+} doping. The magnetic properties of $\text{YMn}_{1-x}\text{Fe}_x\text{O}_3$ samples are significantly enhanced, and can be attributed to doping Fe^{3+} ion in YMnO_3 . According to XRD patterns, it can be obtained that the lattice structures of $\text{YMn}_{1-x}\text{Fe}_x\text{O}_3$ ($0 < x < 0.1$)

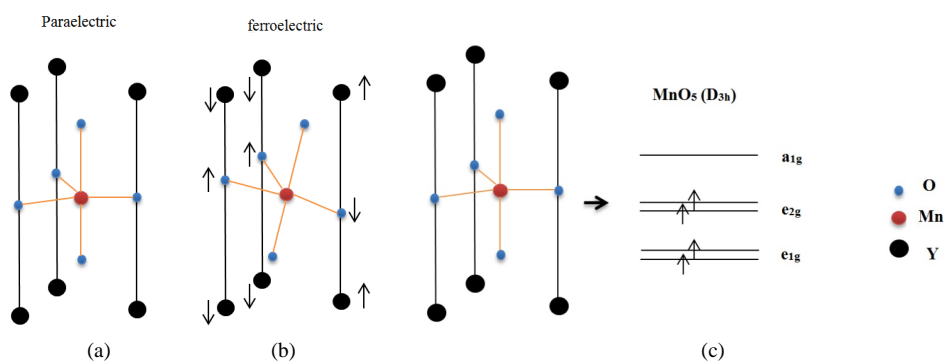


Figure 4. (a) Crystal structure of hexagonal of YMnO_3 with paraelectric phase; (b) Crystal structure of hexagonal of YMnO_3 with ferroelectric phase; (c) Schematic crystal field splittings for MnO_5 (D_{3h}).

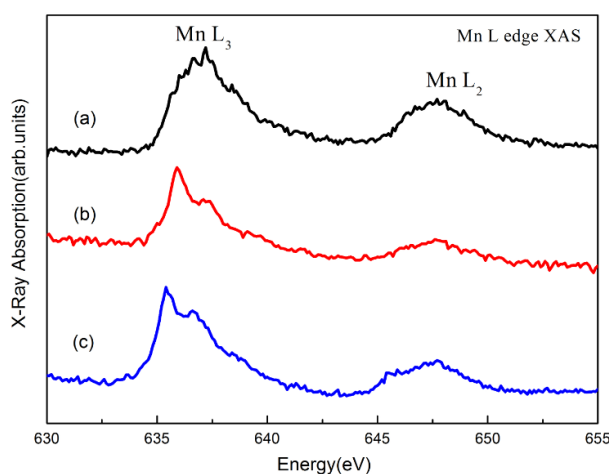


Figure 5. The X-ray absorption spectroscopy (XAS) of Mn L edge of $\text{YMn}_{1-x}\text{Fe}_x\text{O}_3$ ($0 < x < 0.1$) samples. (a) $x = 0$; (b) $x = 0.05$; (c) $x = 0.08$.

samples slightly shrink. Based on O K edge and Mn L edge XAS absorption spectra of $\text{YMn}_{1-x}\text{Fe}_x\text{O}_3$ ($0 < x < 0.1$) samples, it can be obtained that distortion occurs on the surrounded ligand structures of Y^{3+} and Mn^{3+} and that the orbital hybridization of Y-O and Mn-O are enhanced as Fe^{3+} ions doped, explaining the magnetic enhancement of $\text{YMn}_{1-x}\text{Fe}_x\text{O}_3$ ($0 < x < 0.1$) samples.

Acknowledgements

This work is supported by the National Natural Science Foundation of China (U1232133). We are in debt to photoemission spectroscopy experiment station of Beijing Synchrotron Radiation Facility for their help in measuring the XAS spectra.

References

- [1] Spaldin, N.A. and Fiebig, M. (2005) *Science*, **309**, 391. <http://dx.doi.org/10.1126/science.1113357>
- [2] Serrao, C.R., Krupanidhi, S.B., Bhattacharjee, J., Waghmare, U.V., Kundu, A.K. and Rao, C.N.R. (2006) *J. Appl. Phys.*, **100**, 076104. <http://dx.doi.org/10.1063/1.2356093>
- [3] Lee, S., Pirogov, A., Han, J.H., Park, J.G., Hoshikawa, A. and KaMiyama, T. (2005) *Phys. Rev. B*, **71**, 180413. <http://dx.doi.org/10.1103/PhysRevB.71.180413>
- [4] Nugroho, A., Bellido, N., Adem, U., Nenert, G., Simon, Ch., Tjia, M.O., Mostovoy, M. and Palstra, T.T.M. (2007) *Phys. Rev. B*, **75**, 174435. <http://dx.doi.org/10.1103/PhysRevB.75.174435>
- [5] Chatterjee, S. and Nigam, A.K. (2002) *Phys. Rev. B*, **66**, 104403. <http://dx.doi.org/10.1103/PhysRevB.66.104403>
- [6] Park, J. and Lee, S. (2010) *Phys. Rev. B*, **82**, 054428. <http://dx.doi.org/10.1103/PhysRevB.82.054428>
- [7] Asokan, K., Chen, Y.S., Pao, C.W., Tsai, H.M., Lee, C.W.O., Lin, C.H., Hsueh, H.C., *et al.* (2009) *Appl. Phys. Lett.*, **95**, 131901. <http://dx.doi.org/10.1063/1.3224905>
- [8] Namdeo, S., Sinha, A.K., Singh, M.N. and Awasthi, A.M. (2013) *J. Appl. Phys.*, **113**, 104101. <http://dx.doi.org/10.1063/1.4794831>
- [9] Asaka, T., Nemoto, K., Kimoto, K., Arima, T. and Matsui, Y. (2005) *Phys. Rev. B*, **71**, 014114. <http://dx.doi.org/10.1103/PhysRevB.71.014114>
- [10] Park, J., Kang, M., Kim, J., Lee, S., Jang, K.H., Pirogov, A., Park, J.G., *et al.* (2009) *Phys. Rev. B*, **79**, 064417. <http://dx.doi.org/10.1103/PhysRevB.79.064417>
- [11] Yoo, Y.J., Lee, Y.P., Park, J.S., Kang, J.H., Kim, J., Lee, B.W. and Seo, M.S. (2012) *J. Appl. Phys.*, **112**, 013903. <http://dx.doi.org/10.1063/1.4731631>
- [12] Cho, D.Y., Kim, J.Y., Park, B.G., Rho, K.J., Park, J.H., Noh, H.J., *et al.* (2007) *Phys. Rev. Lett.*, **98**, 217601. <http://dx.doi.org/10.1103/PhysRevLett.98.217601>
- [13] Van Aken, B.B., Palstra, T.T.M., *et al.* (2004) *Nat. Mater.*, **3**, 164. <http://dx.doi.org/10.1038/nmat1080>